



CERN-EP-2025-019
 LHCb-PAPER-2024-055
 February 26, 2025

Observation of a new charmed baryon decaying to $\Xi_c^+\pi^-\pi^+$

LHCb collaboration[†]

Abstract

The $\Xi_c^+\pi^-\pi^+$ spectrum is investigated using proton-proton collisions at a center-of-mass energy of 13 TeV, corresponding to an integrated luminosity of 5.4 fb^{-1} , collected by the LHCb experiment during 2016–2018. Four states are observed with high significance, and their masses and widths are measured to be

$$m[\Xi_c(2815)^+] = 2816.65 \pm 0.03 \pm 0.03 \pm 0.23 \text{ MeV},$$

$$\Gamma[\Xi_c(2815)^+] = 2.07 \pm 0.08 \pm 0.12 \text{ MeV},$$

$$m[\Xi_c(2923)^+] = 2922.8 \pm 0.3 \pm 0.5 \pm 0.2 \text{ MeV},$$

$$\Gamma[\Xi_c(2923)^+] = 5.3 \pm 0.9 \pm 1.4 \text{ MeV},$$

$$m[\Xi_c(2970)^+] = 2968.6 \pm 0.5 \pm 0.5 \pm 0.2 \text{ MeV},$$

$$\Gamma[\Xi_c(2970)^+] = 31.7 \pm 1.7 \pm 1.9 \text{ MeV},$$

$$m[\Xi_c(3080)^+] = 3076.8 \pm 0.7 \pm 1.3 \pm 0.2 \text{ MeV},$$

$$\Gamma[\Xi_c(3080)^+] = 6.8 \pm 2.3 \pm 0.9 \text{ MeV},$$

where the uncertainties are statistical, systematic, and due to the limited precision on the Ξ_c^+ mass, respectively. The $\Xi_c(2923)^+$ baryon is observed for the first time, and is consistent with being the isospin partner of the previously observed $\Xi_c(2923)^0$ state. Most of the measured parameters are more precise than existing world averages.

Submitted to Phys. Rev. Lett.

© 2025 CERN for the benefit of the LHCb collaboration. [CC BY 4.0 licence](#).

[†]Authors are listed at the end of this paper.

Singly charmed baryons are bound states of a charm quark (c) and two light quarks (u , d or s). Due to the large mass difference between the charm and the lighter quarks, these baryons provide an insight into the spectrum of hadronic states using symmetries described by the Heavy Quark Effective Theory [1, 2]. Numerous theoretical predictions of the properties of heavy baryons, containing either a charm or a beauty quark, have been made in recent years [3–22], including some based on Lattice QCD calculations [23–26]. There are fifteen singly charmed baryons with orbital angular momentum $L = 0$, all of which have now been observed [27]. The number increases drastically when considering the orbital and radial excitations. Modeling such states as a heavy quark interacting with a light diquark can help restrict the number of possible physical states [16, 20]. However, despite the progress made in recent years, this number remains much higher than that observed experimentally [28–33]. This implies that many other states remain undiscovered or that some configurations are forbidden by selection rules. The latter would have a broad impact in hadron spectroscopy given that the diquark is also used as a building block of exotic states, including tetraquarks and pentaquarks [34–36].

The Ξ_c baryons, states with quark content csu or csd , are described by a wave function which is antisymmetric (*e.g.* the Ξ_c ground state) or symmetric (*e.g.* Ξ'_c or $\Xi_c(2645)$ excitations) under interchange of the light quark flavors. More than one hundred excited Ξ_c baryons are expected in the mass region 2.8–3.8 GeV [23] and the mass splitting between the states can be so small, relative to their natural widths, that they are difficult to resolve experimentally.¹ This might be the case for the $\Xi_c(2970)$ state whose natural width was measured to be about 30 MeV in the $\Xi'_c \pi$ and $\Xi_c \pi^+ \pi^-$ spectra [37] while only 15 MeV in the $\Lambda_c^+ K^- \pi^+$ [38] and $\Lambda_c^+ K^-$ [32] systems. More precise measurements are needed to determine if two different Ξ_c baryons have been mistakenly identified as a single state due to the proximity of their masses.

This Letter presents a search for excited Ξ_c^+ baryons, hereafter collectively termed Ξ_c^{**+} , in the $\Xi_c^+ \pi^- \pi^+$ spectrum. This final state was studied by the Belle collaboration, which reported the observation of the $\Xi_c(2815)^+$ and $\Xi_c(2970)^+$ baryons [37]. The spin-parity of the latter was also measured to be $J^P = \frac{1}{2}^+$ [39]. A further structure peaking at around 2.92 GeV was noted, although it was not statistically significant.

Data used in this analysis were collected by the LHCb experiment during 2016–2018 from proton-proton (pp) collisions at a center-of-mass energy of 13 TeV, corresponding to an integrated luminosity of 5.4 fb^{-1} . Excited Ξ_c^+ states are reconstructed through their intermediate decay to $\Xi_c(2645)^0 \pi^+$, with $\Xi_c(2645)^0 \rightarrow \Xi_c^+ \pi^-$ and $\Xi_c^+ \rightarrow p K^- \pi^+$.²

The LHCb detector [40, 41] is a single-arm forward spectrometer covering the pseudorapidity range $2 < \eta < 5$, designed for the study of particles containing b or c quarks. The detector elements particularly relevant to this analysis are: a silicon-strip vertex detector surrounding the pp interaction region that allows c and b hadrons to be identified from their characteristically long flight distance [42]; a large-area silicon-strip detector located upstream of a dipole magnet with a bending power of about 4 T m, and three stations of silicon-strip detectors and straw drift tubes [43] placed downstream of the magnet; and two ring-imaging Cherenkov detectors that provide particle identification (PID) information to discriminate between different species of charged hadrons [44]. The online event selection is performed by a trigger [45] consisting of a hardware stage based

¹Natural units with $\hbar = c = 1$ are used throughout.

²The inclusion of charge-conjugate processes is implied throughout.

on information from the calorimeter and muon systems, followed by a two-level software stage which applies a full event reconstruction.

Simulation is used in this analysis to optimize the event selection and to model the experimental mass resolution. Proton-proton collisions are generated using PYTHIA [46] with a specific LHCb configuration [47]. Decays of unstable particles are described by EVTGEN [48]. The interaction of the generated particles with the detector, and its response, are implemented using the GEANT4 toolkit [49] as described in Ref. [50].

In order to maximize the signal efficiency, no explicit requirements are imposed at the hardware trigger stage. At the software trigger stage a dedicated algorithm reconstructs $\Xi_c^+ \rightarrow pK^-\pi^+$ candidates from the combination of three reconstructed tracks which must fulfill loose kinematic and PID requirements and be consistent with originating from a common vertex with significant displacement from any primary interaction vertex (PV) in the event. The Ξ_c^+ candidate must have a measured lifetime with respect to the associated PV exceeding 0.15 ps, and a mass in the range $2432.5 < m(pK^-\pi^+) < 2502.5$ MeV.

The Ξ_c^+ candidates selected by the trigger are subsequently combined with a pair of oppositely charged particles, fulfilling loose pion PID requirements and consistent with originating from the Ξ_c^+ associated PV, to form $\Xi_c^{**+} \rightarrow \Xi_c(2645)^0 (\rightarrow \Xi_c^+\pi^-)\pi^+$ candidates. The $\Xi_c^+\pi^-\pi^+$ system must form a good-quality vertex and satisfy the reconstructed mass conditions $m(\Xi_c^+\pi^-\pi^+) < 3300$ MeV and $[m(\Xi_c^+\pi^-) - m(\Xi_c^+) - m_{\pi^-}^{\text{PDG}}] < 150$ MeV, where the second condition selects the $\Xi_c(2645)^0$ resonance region and $m_{\pi^-}^{\text{PDG}}$ is the known pion mass [27].

Three selection stages are performed to sequentially optimize the signal for Ξ_c^+ , $\Xi_c(2645)^0$, and Ξ_c^{**+} states. In the first (Ξ_c^+) selection stage, a series of loose criteria are initially imposed to reduce the dominant combinatorial background by 85% while retaining 83% of the signal. These include a requirement on the alignment of the Ξ_c^+ momentum with the direction determined by its production and decay vertices, PID requirements on each final-state particle, and loose requirements on topological variables related to the Ξ_c^+ flight distance and its consistency with originating from a PV.

To further suppress background in the Ξ_c^+ sample, a multivariate algorithm (MVA) is trained with signal and background samples extracted using the *sPlot* technique [51]. The Ξ_c^+ mass distribution is fitted to obtain weights for signal and background, based on a 5% random sampling of the full data sample. In this fit the signal is described by a double Gaussian function, *i.e.* the sum of two Gaussian functions constrained to have a common mean, and the background by a first-order polynomial function. A cross-validation method is used to ensure the classifier is not applied to the data on which it is trained. A feed-forward neural network [52, 53] is configured with a loss function that properly accounts for the weights in the training samples [54]. A total of 29 input variables are included, mainly topological quantities and PID variables for the final-state particles. Following the training, a requirement is imposed on the classifier output to maximize the signal significance $S/\sqrt{S + B}$, where S (B) is the signal (background) yield. This selection retains 84% (16%) of the signal (background). The resulting $m(pK^-\pi^+)$ distribution, after imposing all Ξ_c^+ selection criteria, is shown in Fig. 1 for the full data sample. Also shown is an indicative fit using the same model as described above. For subsequent analysis a tighter mass window of $2451.3 < m(pK^-\pi^+) < 2486.0$ MeV is imposed, containing 98% of the signal. Around 7.7×10^6 Ξ_c^+ signal candidates are selected, with a purity of 84%.

In the second selection stage, a separate classifier is trained to optimize the signal significance of the $\Xi_c(2645)^0$ state. The signal and background training samples are

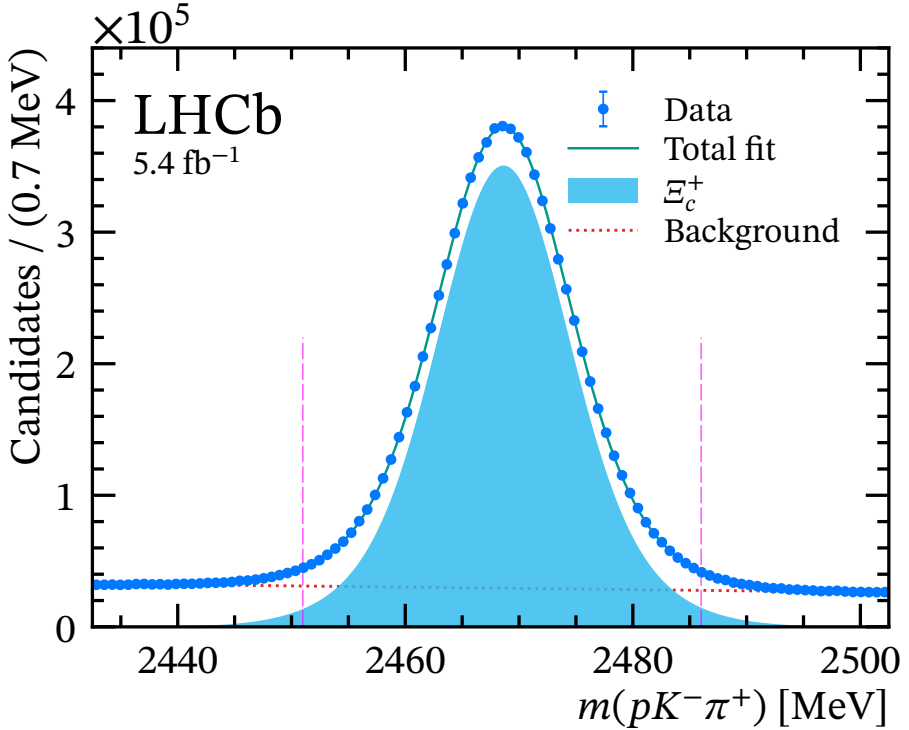


Figure 1: Distribution of $m(pK^-\pi^+)$ for candidates passing Ξ_c^+ selection requirements, together with the fit model. The dashed vertical lines delimit the mass window imposed for subsequent selection stages.

again derived from cross-validated data using the *sPlot* technique [51], following a fit to the quantity $m_{\text{corr}}[\Xi_c(2645)^0] \equiv m(\Xi_c^+\pi^-) - m(\Xi_c^+) + m_{\Xi_c^+}^{\text{PDG}}$, where the final entry corresponds to the known Ξ_c^+ mass [27]. Using this mass difference leads to improved resolution and, hence, higher signal purity. In the fit, the $\Xi_c(2645)^0$ signal peak is described by the convolution of a relativistic Breit–Wigner (RBW) function with a double Gaussian resolution function. Simulation is used to fix the parameters of the resolution function, with both widths free to vary in the fit through a common scale factor to account for possible mismodeling. The dominant background is combinatorial, either from genuine Ξ_c^+ baryons combined with an unrelated track, or fake Ξ_c^+ candidates. These components are described empirically by a function $f(x) = a(x - m_0)^k + b(x - m_0)$ with a , b , k , and m_0 as free parameters. Two additional peaking backgrounds are observed in the sample. The first occurs close to the signal peak, originating from $\Xi_c(2815)^0 \rightarrow \Xi_c(2645)^+(\rightarrow \Xi_c^+\pi^0)\pi^-$ decays, where the neutral pion is not reconstructed. The second occurs in the mass region around 2680 MeV, due to $\Xi_c(2790)^0 \rightarrow \Xi_c^{'+}(\rightarrow \Xi_c^+\gamma)\pi^-$ decays with the photon not reconstructed. Both of these partially reconstructed backgrounds are described using templates derived from a fast simulation software [55]. Their mass positions are allowed to shift through Gaussian constraints centered on zero and with widths 0.3 MeV and 0.5 MeV for the $\Xi_c(2815)^0$ and $\Xi_c(2790)^0$ decays, respectively, based on the experimental mass uncertainties of these states [27].

The weighted signal and background samples obtained from the *sPlot* fit are used to train a gradient Boosted Decision Tree (BDT) [56–58] with 14 input variables, one of which

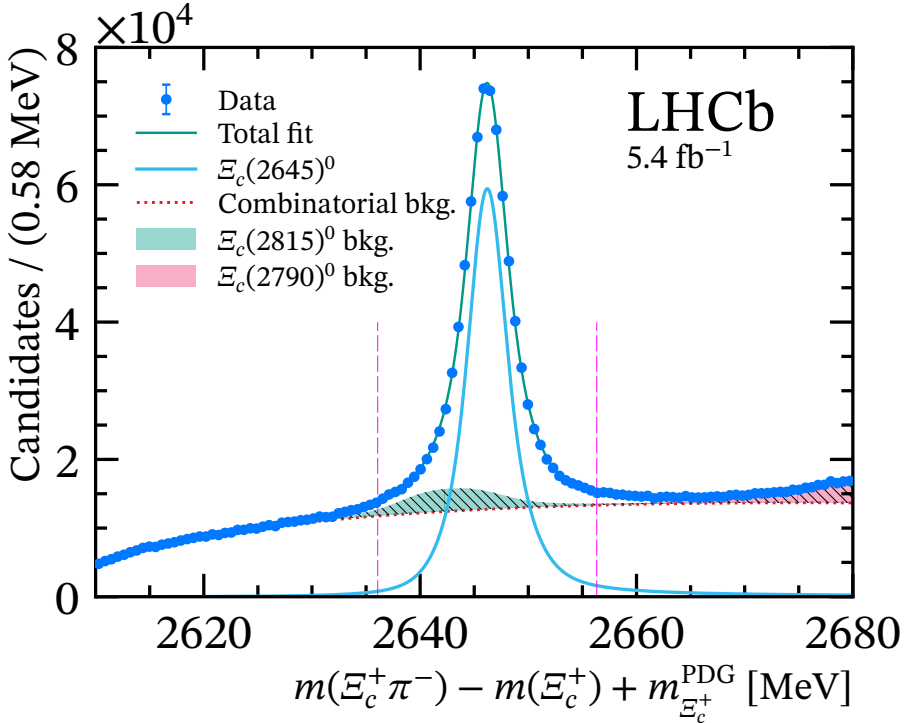


Figure 2: Distribution of $m_{\text{corr}}(\Xi_c(2645)^0)$ for candidates passing the second selection stage. The fit model is also shown for illustrative purposes. The dashed vertical lines enclose the mass region selected for subsequent analysis.

is the neural network output from the first selection stage. The other variables include PID and kinematic quantities for the pion, and topological quantities characterizing the $\Xi_c^+\pi^-$ vertex quality. A requirement is imposed on the BDT output to optimize the signal significance, which gives a signal (background) retention of 95% (74%). A mass requirement $2635 < m_{\text{corr}}[\Xi_c(2645)^0] < 2656$ MeV is then applied, containing 98% of the signal candidates. In total, around 56.5×10^4 $\Xi_c(2645)^0$ signal candidates are selected, with a purity of 52%. The mass distribution after all criteria have been imposed is shown in Fig. 2 along with the results of an illustrative fit with the same model as described above.

The final selection stage uses a third MVA to optimize possible Ξ_c^{**+} signal peaks in an unbiased way. Simulation is used as a proxy for the signal to train the classifier, with four samples generated with Ξ_c^{**+} mass assignments 2815, 2923, 2970, and 3055 MeV. The input variable distributions and classifier performance are similar for the different mass values, so these four samples are combined in the training. The background proxy sample is taken from data, combining the wrong-sign final states $\Xi_c^+\pi^+\pi^+$ and $\Xi_c^+\pi^-\pi^-$, which is found to provide a good description of the background entering the signal sample. A gradient BDT [59] is trained with 15 input variables covering kinematic, topological, and PID quantities. Following training, a requirement on the BDT output is imposed to maximize the quantity $\varepsilon/(5/2 + \sqrt{B})$ [60] where ε is the signal efficiency taken from simulation and B is the background yield under the signal peak of interest, taken from the wrong-sign sample. The optimal requirement is calculated separately for the four

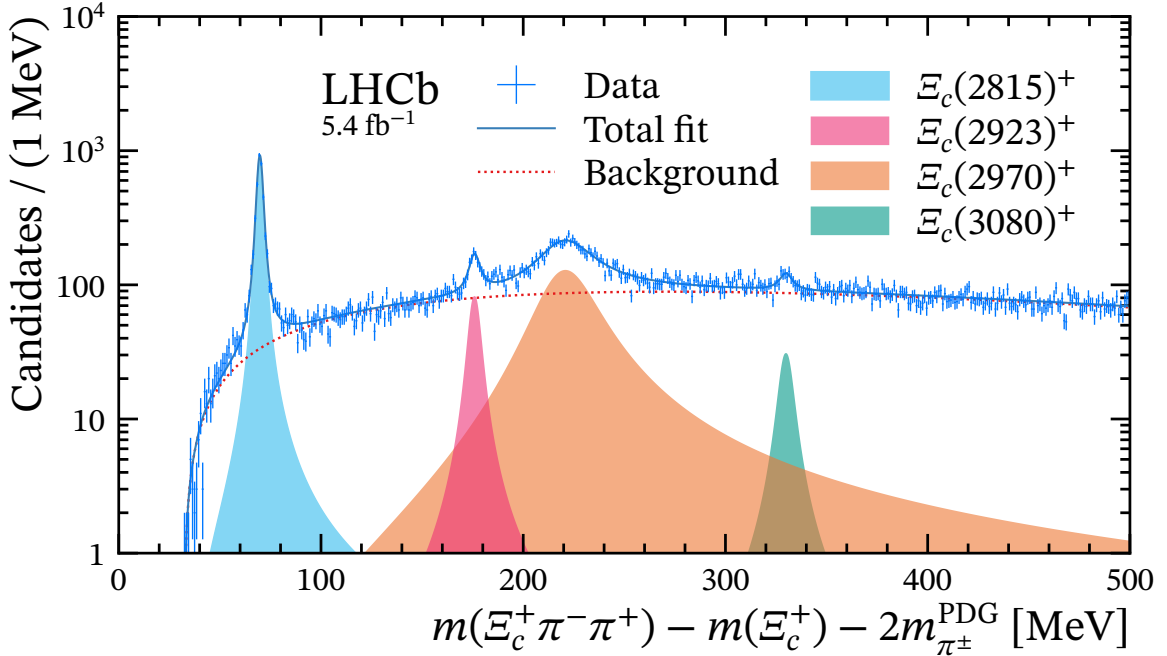


Figure 3: Distribution of ΔM for candidates passing all selection requirements, shown with the fit model. The individual signal components for the four observed states are drawn separately as filled curves, and the background as a dotted line.

mass assignments used in simulation, and exhibits a weak mass dependence. The chosen requirement is based on the $\Xi_c(2923)^+$ hypothesis, and retains 34% (0.7%) of signal (background) in the proxy samples.

A final requirement is imposed to reject cases where a single particle is reconstructed as two tracks, with both included in the final state. Such candidates are removed by requiring the two-dimensional angular separation between all pairs of final-state particles to exceed 0.08 mrad. Following the application of all selection criteria, 84% of events include only one selected Ξ_c^{**+} candidate. For events with multiple candidates, all are accepted, with an alternative treatment considered later as a cross-check.

The mass distribution for candidates passing all selection requirements is shown in Fig. 3, expressed in terms of the mass difference $\Delta M \equiv m(\Xi_c^+\pi^-\pi^+) - m(\Xi_c^+) - 2m_{\pi^\pm}^{\text{PDG}}$. Four distinct peaks are observed above a smooth background rising from the kinematic threshold. These peaks are labeled as $\Xi_c(2815)^+$, $\Xi_c(2923)^+$, $\Xi_c(2970)^+$, and $\Xi_c(3080)^+$ based on their proximity to existing states [27], or in the case of $\Xi_c(2923)^+$ to the corresponding neutral state observed in decays to $\Lambda_c^+ K^-$ [32].

An extended unbinned maximum-likelihood fit is performed on the ΔM distribution to determine the masses and widths of these states, and their statistical significances. In this fit, the background is described by an empirical function $f(x) = x^k \exp(-cx)$, where $x \equiv (\Delta M - m_0)$, and k , c , and m_0 are free parameters. This model choice is motivated by studies of the wrong-sign samples. Each signal peak is described by the convolution of a relativistic Breit–Wigner function with a resolution function obtained from simulation. Different assumptions are tested for the Blatt–Weisskopf barrier factors [61] and orbital angular momentum of the states, with the results used to assign systematic uncertainties

as described later. The resolution function is determined using the four simulated Ξ_c^{**+} samples, which correspond quite closely in mass to the states observed in data. The ΔM resolution is determined from simulation, and is described by a double Gaussian function with a mass-dependent scale factor applied to both widths. This resolution varies from 1 MeV for the $\Xi_c(2815)^+$ state to 2.5 MeV for the $\Xi_c(3080)^+$ state.

The free parameters of the ΔM fit are the yields (N), peak positions, and widths (Γ) of each of the four signal peaks, the three background shape parameters, and the background yield. The absolute masses (m) are then determined from the peak positions in ΔM by adding the known Ξ_c^+ and π^\pm masses [27]. The fit model provides a good description of the data, with a χ^2 of 478 for 458 degrees of freedom. The parameters for the observed states are measured to be

$$\begin{aligned} N[\Xi_c(2815)^+] &= 4072 \pm 77, \\ m[\Xi_c(2815)^+] &= 2816.65 \pm 0.03 \pm 0.03 \pm 0.23 \text{ MeV}, \\ \Gamma[\Xi_c(2815)^+] &= 2.07 \pm 0.08 \pm 0.12 \text{ MeV}, \\ N[\Xi_c(2923)^+] &= 738 \pm 76, \\ m[\Xi_c(2923)^+] &= 2922.8 \pm 0.3 \pm 0.5 \pm 0.2 \text{ MeV}, \\ \Gamma[\Xi_c(2923)^+] &= 5.3 \pm 0.9 \pm 1.4 \text{ MeV}, \\ N[\Xi_c(2970)^+] &= 6105 \pm 255, \\ m[\Xi_c(2970)^+] &= 2968.6 \pm 0.5 \pm 0.5 \pm 0.2 \text{ MeV}, \\ \Gamma[\Xi_c(2970)^+] &= 31.7 \pm 1.7 \pm 1.9 \text{ MeV}, \\ N[\Xi_c(3080)^+] &= 344 \pm 77, \\ m[\Xi_c(3080)^+] &= 3076.8 \pm 0.7 \pm 1.3 \pm 0.2 \text{ MeV}, \\ \Gamma[\Xi_c(3080)^+] &= 6.8 \pm 2.3 \pm 0.9 \text{ MeV}, \end{aligned}$$

where the first uncertainty is statistical, the second is due to experimental systematic effects discussed below, and the third uncertainty on the masses is from the limited knowledge of the Ξ_c^+ mass [27].

The statistical significance for the two lowest-yield peaks is determined from Wilks' theorem [62]. The $\Xi_c(2923)^+$ state is observed with over 10σ significance, representing the discovery of this state. The $\Xi_c(3080)^+$ state is observed with 5.4σ significance. To account for possible systematic effects from the choice of signal and background model, the calculation is repeated for the alternative model choices described below, and the lowest significance is quoted.

Various sources of systematic uncertainty are considered for the mass and width measurements, as summarized in Table 1. Alternative descriptions of the signal peaks are tested by varying the Blatt–Weisskopf radius used in the RBW function from its baseline value of 3.1 GeV^{-1} to 2.0 GeV^{-1} and 4.0 GeV^{-1} . In addition, the assumed orbital angular momentum of the decay products, L , is varied independently for all four observed states to cover any physically allowed values between $L = 0$ and $L = 2$. The standard deviation of each signal parameter across the full ensemble of alternative signal models is taken as a systematic uncertainty (labeled *RBW* in Table 1). In the baseline fit no interference is included between the observed states. The $\Xi_c(2970)^+$ resonance has a significant overlap with both the $\Xi_c(2923)^+$ and $\Xi_c(3080)^+$ peaks, and so any interference could influence

Table 1: Summary of uncertainties on all measured parameters (in MeV), including a breakdown of systematic uncertainties as described in the text. Entries marked with a dash are not relevant for that measurement.

Contribution	$\Xi_c(2815)^+$		$\Xi_c(2923)^+$		$\Xi_c(2970)^+$		$\Xi_c(3080)^+$	
	m	Γ	m	Γ	m	Γ	m	Γ
RBW	0.00	0.02	0.09	1.12	0.15	0.55	0.02	0.68
Interference	0.00	0.01	0.53	0.70	0.44	1.05	1.26	0.65
Resolution	0.00	0.12	0.00	0.11	0.01	0.04	0.00	0.08
Background	0.00	0.01	0.01	0.32	0.11	1.51	0.04	0.08
Mom. scale	0.02	—	0.05	—	0.07	—	0.10	—
Energy loss	0.02	—	0.02	—	0.02	—	0.02	—
Sel. bias	0.02	—	0.02	—	0.02	—	0.02	—
Total syst.	0.03	0.12	0.54	1.36	0.48	1.92	1.27	0.95
Stat.	0.03	0.08	0.28	0.87	0.46	1.68	0.72	2.28

the measured parameters. This is tested by performing two additional fits, independently allowing interference between each pair of adjacent states, and assigning a systematic uncertainty equal to the maximum shift in each parameter compared to the baseline result (*Interference*).

Potential mismodeling of the detector resolution in simulation is tested by multiplying the Gaussian widths for all resolution functions by a scale factor of 0.9 or 1.1 and repeating the fits. This range is chosen based on detailed studies of the $\Xi_c^+(2645)$ peak in data and simulation. Systematic uncertainties on fit parameters are then assigned as their maximum shifts (*Resolution*). The description of the background component in the fit to the Δm distribution is varied by using a third-order polynomial function, and associated systematic uncertainties are assigned as the shift in fit parameters from their baseline values (*Background*).

The mass measurements may be affected by the LHCb momentum scale calibration (*Mom. scale*) and by mismodeling of material leading to incorrect energy loss assumptions in simulation and particle reconstruction (*Energy loss*). Previous studies indicate that the former effect is associated with a systematic uncertainty corresponding to 0.03% of the Q-value for the decay [63]. The systematic uncertainty due to imperfect modeling of the energy loss is assigned as 0.02 MeV for all mass measurements, corresponding to 0.01 MeV for each of the two pion tracks entering the ΔM calculation [63]. The impact from other final-state particles cancels in the mass difference. In addition, a potential bias in the mass measurements originating from the event selection is tested by comparing the reconstructed masses in simulation before and after the offline selection requirements are imposed. A small shift of 0.016 MeV is found, consistent for all four states, which is assigned as a systematic uncertainty (*Sel. bias*). No correction is applied as this shift is found to be compatible with zero.

Several cross-checks are performed to confirm the robustness of the results. The fit is repeated separately for each of the two Ξ_c^\pm charges, for each of the two LHCb dipole magnet polarities, and for each of the three data-taking years. In all cases the results are self-consistent. Fits are also performed with additional resonances allowed to contribute,

namely $\Xi_c(2939)^+$, $\Xi_c(3055)^+$, and $\Xi_c(3123)^+$ states. These are added individually to the fit, with their masses and widths constrained from external measurements [27]. In all cases the results are stable compared to the baseline fit, and no evidence is found for the presence of these extra states in the data sample.

In conclusion, this Letter presents a search for excited Ξ_c^+ states decaying to $\Xi_c(2645)^0\pi^+$, with $\Xi_c(2645)^0 \rightarrow \Xi_c^+\pi^-$ and $\Xi_c^+ \rightarrow pK^-\pi^+$. Four states are observed with high significance, including the discovery of the $\Xi_c(2923)^+$ baryon, and the first observation of the $\Xi_c(3080)^+$ baryon in this final state. Masses and widths are measured for all four states, and are competitive with, or more precise than the existing world averages. The natural width of the $\Xi_c(2970)^+$ state is not consistent with that of the $\Xi_c(2965)^0$ baryon observed in the $\Lambda_c^+K^-$ mass spectrum [32], indicating that the two are different excited Ξ_c states. This continues the success of the LHCb experiment in discovering new hadronic states and precisely measuring their properties, a key input for understanding QCD in the nonperturbative realm.

Acknowledgements

We express our gratitude to our colleagues in the CERN accelerator departments for the excellent performance of the LHC. We thank the technical and administrative staff at the LHCb institutes. We acknowledge support from CERN and from the national agencies: ARC (Australia); CAPES, CNPq, FAPERJ and FINEP (Brazil); MOST and NSFC (China); CNRS/IN2P3 (France); BMBF, DFG and MPG (Germany); INFN (Italy); NWO (Netherlands); MNiSW and NCN (Poland); MCID/IFA (Romania); MICIU and AEI (Spain); SNSF and SER (Switzerland); NASU (Ukraine); STFC (United Kingdom); DOE NP and NSF (USA). We acknowledge the computing resources that are provided by ARDC (Australia), CBPF (Brazil), CERN, IHEP and LZU (China), IN2P3 (France), KIT and DESY (Germany), INFN (Italy), SURF (Netherlands), Polish WLCG (Poland), IFIN-HH (Romania), PIC (Spain), CSCS (Switzerland), and GridPP (United Kingdom). We are indebted to the communities behind the multiple open-source software packages on which we depend. Individual groups or members have received support from Key Research Program of Frontier Sciences of CAS, CAS PIFI, CAS CCEPP, Fundamental Research Funds for the Central Universities, and Sci. & Tech. Program of Guangzhou (China); Minciencias (Colombia); EPLANET, Marie Skłodowska-Curie Actions, ERC and NextGenerationEU (European Union); A*MIDEX, ANR, IPhU and Labex P2IO, and Région Auvergne-Rhône-Alpes (France); Alexander-von-Humboldt Foundation (Germany); ICSC (Italy); Severo Ochoa and María de Maeztu Units of Excellence, GVA, XuntaGal, GENCAT, InTalent-Inditex and Prog. Atracción Talento CM (Spain); SRC (Sweden); the Leverhulme Trust, the Royal Society and UKRI (United Kingdom).

End Matter

In the fit to the ΔM distribution, the peak positions are free parameters, denoted $\delta M(X)$ for state X . The values returned by the fit are

$$\begin{aligned}\delta M[\Xi_c(2815)^+] &= 69.80 \pm 0.03 \pm 0.03 \text{ MeV}, \\ \delta M[\Xi_c(2923)^+] &= 175.95 \pm 0.28 \pm 0.54 \text{ MeV}, \\ \delta M[\Xi_c(2970)^+] &= 221.77 \pm 0.46 \pm 0.48 \text{ MeV}, \\ \delta M[\Xi_c(3080)^+] &= 329.92 \pm 0.72 \pm 1.27 \text{ MeV},\end{aligned}$$

where the first uncertainty is statistical and the second is due to experimental systematic effects. These measurements are converted into absolute mass measurements for the excited baryons, as reported in the paper, by adding the masses of the two charged pions and the Ξ_c^+ baryon (2467.71 ± 0.23 MeV) taken from Ref. [27].

References

- [1] A. G. Grozin, *Introduction to the heavy quark effective theory. Part 1*, [arXiv:hep-ph/9908366](https://arxiv.org/abs/hep-ph/9908366).
- [2] T. Mannel, *Effective theory for heavy quarks*, *Lect. Notes Phys.* **479** (1997) 387, [arXiv:hep-ph/9606299](https://arxiv.org/abs/hep-ph/9606299).
- [3] S. Migura, D. Merten, B. Metsch, and H.-R. Petry, *Charmed baryons in a relativistic quark model*, *Eur. Phys. J.* **A28** (2006) 41, [arXiv:hep-ph/0602153](https://arxiv.org/abs/hep-ph/0602153).
- [4] D. Ebert, R. N. Faustov, and V. O. Galkin, *Masses of excited heavy baryons in the relativistic quark-diquark model*, *Phys. Lett.* **B659** (2008) 612, [arXiv:0705.2957](https://arxiv.org/abs/0705.2957).
- [5] W. Roberts and M. Pervin, *Heavy baryons in a quark model*, *Int. J. Mod. Phys.* **A23** (2008) 2817, [arXiv:0711.2492](https://arxiv.org/abs/0711.2492).
- [6] H. Garcilazo, J. Vijande, and A. Valcarce, *Faddeev study of heavy baryon spectroscopy*, *J. Phys.* **G34** (2007) 961, [arXiv:hep-ph/0703257](https://arxiv.org/abs/hep-ph/0703257).
- [7] A. Valcarce, H. Garcilazo, and J. Vijande, *Towards an understanding of heavy baryon spectroscopy*, *Eur. Phys. J.* **A37** (2008) 217, [arXiv:0807.2973](https://arxiv.org/abs/0807.2973).
- [8] D. Ebert, R. N. Faustov, and V. O. Galkin, *Spectroscopy and Regge trajectories of heavy baryons in the relativistic quark-diquark picture*, *Phys. Rev.* **D84** (2011) 014025, [arXiv:1105.0583](https://arxiv.org/abs/1105.0583).
- [9] J. Vijande, A. Valcarce, T. F. Caramés, and H. Garcilazo, *Heavy hadron spectroscopy: A quark model perspective*, *Int. J. Mod. Phys.* **E22** (2013) 1330011, [arXiv:1212.4383](https://arxiv.org/abs/1212.4383).
- [10] T. Yoshida *et al.*, *Spectrum of heavy baryons in the quark model*, *Phys. Rev.* **D92** (2015) 114029, [arXiv:1510.01067](https://arxiv.org/abs/1510.01067).
- [11] H.-X. Chen *et al.*, *P-wave charmed baryons from QCD sum rules*, *Phys. Rev.* **D91** (2015) 054034, [arXiv:1502.01103](https://arxiv.org/abs/1502.01103).
- [12] Z. Shah, K. Thakkar, A. K. Rai, and P. C. Vinodkumar, *Mass spectra and Regge trajectories of Λ_c^+ , Σ_c^0 , Ξ_c^0 and Ω_c^0 baryons*, *Chin. Phys.* **C40** (2016) 123102, [arXiv:1609.08464](https://arxiv.org/abs/1609.08464).
- [13] H.-X. Chen *et al.*, *D-wave charmed and bottomed baryons from QCD sum rules*, *Phys. Rev.* **D94** (2016) 114016, [arXiv:1611.02677](https://arxiv.org/abs/1611.02677).
- [14] J. Oudichhya, K. Gandhi, and A. K. Rai, *Ground and excited state masses of Ω_c^0 , Ω_{cc}^+ and Ω_{ccc}^{++} baryons*, *Phys. Rev.* **D103** (2021) 114030, [arXiv:2105.10647](https://arxiv.org/abs/2105.10647).
- [15] P. Jakhad, J. Oudichhya, K. Gandhi, and A. K. Rai, *Identification of newly observed singly charmed baryons using the relativistic flux tube model*, *Phys. Rev.* **D108** (2023) 014011, [arXiv:2306.06349](https://arxiv.org/abs/2306.06349).
- [16] H. García-Tecocoatzi *et al.*, *Strong decay widths and mass spectra of charmed baryons*, *Phys. Rev.* **D107** (2023) 034031, [arXiv:2205.07049](https://arxiv.org/abs/2205.07049).

- [17] E. Ortiz-Pacheco and R. Bijker, *Masses and radiative decay widths of S- and P-wave singly, doubly, and triply heavy charm and bottom baryons*, Phys. Rev. **D108** (2023) 054014, [arXiv:2307.04939](#).
- [18] Z.-Y. Li, G.-L. Yu, Z.-G. Wang, and J.-Z. Gu, *Heavy quark dominance in orbital excitation of singly and doubly heavy baryons*, Eur. Phys. J. **C84** (2024) 106, [arXiv:2311.08251](#).
- [19] X.-Z. Weng, W.-Z. Deng, and S.-L. Zhu, *Heavy baryons in the relativized quark model with chromodynamics*, Phys. Rev. **D110** (2024) 056052, [arXiv:2405.19039](#).
- [20] H. García-Tecocoatzi *et al.*, *Strong decay widths and mass spectra of the 1D, 2P and 2S singly bottom baryons*, Phys. Rev. **D110** (2024) 114005, [arXiv:2307.00505](#).
- [21] H.-M. Yang and H.-X. Chen, *P-wave charmed baryons of the SU(3) flavor 6_F*, Phys. Rev. **D104** (2021) 034037, [arXiv:2106.15488](#).
- [22] H.-M. Yang, H.-X. Chen, and Q. Mao, *Excited Ξ_c^0 baryons within the QCD sum rule approach*, Phys. Rev. **D102** (2020) 114009, [arXiv:2004.00531](#).
- [23] M. Padmanath, R. G. Edwards, N. Mathur, and M. Peardon, *Excited-state spectroscopy of singly, doubly and triply-charmed baryons from lattice QCD*, in *Proceedings, 6th International Workshop on Charm Physics (Charm 2013): Manchester, UK, August 31-September 4, 2013*, 2013, [arXiv:1311.4806](#).
- [24] M. Padmanath and N. Mathur, *Quantum numbers of recently discovered Ω_c^0 baryons from lattice QCD*, Phys. Rev. Lett. **119** (2017) 042001, [arXiv:1704.00259](#).
- [25] TWQCD collaboration, Y.-C. Chen and T.-W. Chiu, *Lattice QCD with $N_f = 2+1+1$ domain-wall quarks*, Phys. Lett. **B767** (2017) 193, [arXiv:1701.02581](#).
- [26] TRJQCD collaboration, H. Bahtiyar *et al.*, *Charmed baryon spectrum from lattice QCD near the physical point*, Phys. Rev. **D102** (2020) 054513, [arXiv:2004.08999](#).
- [27] Particle Data Group, S. Navas *et al.*, *Review of particle physics*, Phys. Rev. **D110** (2024) 030001.
- [28] LHCb collaboration, R. Aaij *et al.*, *Study of the $D^0 p$ amplitude in $\Lambda_b^0 \rightarrow D^0 p \pi^-$ decays*, JHEP **05** (2017) 030, [arXiv:1701.07873](#).
- [29] LHCb collaboration, R. Aaij *et al.*, *Observation of five new narrow Ω_c^0 states decaying to $\Xi_c^+ K^-$* , Phys. Rev. Lett. **118** (2017) 182001, [arXiv:1703.04639](#).
- [30] Belle collaboration, J. Yelton *et al.*, *Observation of excited Ω_c charmed baryons in $e^+ e^-$ collisions*, Phys. Rev. **D97** (2018) 051102, [arXiv:1711.07927](#).
- [31] Belle collaboration, Y. B. Li *et al.*, *Observation of $\Xi_c(2930)^0$ and updated measurement of $B^- \rightarrow K^- \Lambda_c^+ \bar{\Lambda}_c^-$ at Belle*, Eur. Phys. J. **C78** (2018) 252, [arXiv:1712.03612](#).
- [32] LHCb collaboration, R. Aaij *et al.*, *Observation of new Ξ_c^0 baryons decaying to $\Lambda_c^+ K^-$* , Phys. Rev. Lett. **124** (2020) 222001, [arXiv:2003.13649](#).

- [33] LHCb collaboration, R. Aaij *et al.*, *Observation of new Ω_c^0 states decaying to the $\Xi_c^+ K^-$ final state*, *Phys. Rev. Lett.* **131** (2023) 131902, [arXiv:2302.04733](https://arxiv.org/abs/2302.04733).
- [34] R. L. Jaffe, *Multiquark hadrons. I. Phenomenology of $Q^2\bar{Q}^2$ mesons*, *Phys. Rev. D* **15** (1977) 267.
- [35] R. L. Jaffe, *Multiquark hadrons. II. Methods*, *Phys. Rev. D* **15** (1977) 281.
- [36] L. Maiani, F. Piccinini, A. D. Polosa, and V. Riquer, *Diquark-antidiquarks with hidden or open charm and the nature of $X(3872)$* , *Phys. Rev. D* **71** (2005) 014028, [arXiv:hep-ph/0412098](https://arxiv.org/abs/hep-ph/0412098).
- [37] Belle collaboration, J. Yelton *et al.*, *Study of excited Ξ_c states decaying into Ξ_c^0 and Ξ_c^+ baryons*, *Phys. Rev. D* **94** (2016) 052011, [arXiv:1607.07123](https://arxiv.org/abs/1607.07123).
- [38] Belle collaboration, Y. Kato *et al.*, *Search for doubly charmed baryons and study of charmed strange baryons at Belle*, *Phys. Rev. D* **89** (2014) 052003, [arXiv:1312.1026](https://arxiv.org/abs/1312.1026).
- [39] Belle collaboration, T. J. Moon *et al.*, *First determination of the spin and parity of the charmed-strange baryon $\Xi_c(2970)^+$* , *Phys. Rev. D* **103** (2021) L111101, [arXiv:2007.14700](https://arxiv.org/abs/2007.14700).
- [40] LHCb collaboration, A. A. Alves Jr. *et al.*, *The LHCb detector at the LHC*, *JINST* **3** (2008) S08005.
- [41] LHCb collaboration, R. Aaij *et al.*, *LHCb detector performance*, *Int. J. Mod. Phys. A* **30** (2015) 1530022, [arXiv:1412.6352](https://arxiv.org/abs/1412.6352).
- [42] R. Aaij *et al.*, *Performance of the LHCb Vertex Locator*, *JINST* **9** (2014) P09007, [arXiv:1405.7808](https://arxiv.org/abs/1405.7808).
- [43] P. d'Argent *et al.*, *Improved performance of the LHCb Outer Tracker in LHC Run 2*, *JINST* **12** (2017) P11016, [arXiv:1708.00819](https://arxiv.org/abs/1708.00819).
- [44] M. Adinolfi *et al.*, *Performance of the LHCb RICH detector at the LHC*, *Eur. Phys. J. C* **73** (2013) 2431, [arXiv:1211.6759](https://arxiv.org/abs/1211.6759).
- [45] R. Aaij *et al.*, *The LHCb trigger and its performance in 2011*, *JINST* **8** (2013) P04022, [arXiv:1211.3055](https://arxiv.org/abs/1211.3055).
- [46] T. Sjöstrand, S. Mrenna, and P. Skands, *A brief introduction to PYTHIA 8.1*, *Comput. Phys. Commun.* **178** (2008) 852, [arXiv:0710.3820](https://arxiv.org/abs/0710.3820); T. Sjöstrand, S. Mrenna, and P. Skands, *PYTHIA 6.4 physics and manual*, *JHEP* **05** (2006) 026, [arXiv:hep-ph/0603175](https://arxiv.org/abs/hep-ph/0603175).
- [47] I. Belyaev *et al.*, *Handling of the generation of primary events in Gauss, the LHCb simulation framework*, *J. Phys. Conf. Ser.* **331** (2011) 032047.
- [48] D. J. Lange, *The EvtGen particle decay simulation package*, *Nucl. Instrum. Meth. A* **462** (2001) 152.

- [49] Geant4 collaboration, J. Allison *et al.*, *Geant4 developments and applications*, *IEEE Trans. Nucl. Sci.* **53** (2006) 270; Geant4 collaboration, S. Agostinelli *et al.*, *Geant4: A simulation toolkit*, *Nucl. Instrum. Meth.* **A506** (2003) 250.
- [50] M. Clemencic *et al.*, *The LHCb simulation application, Gauss: Design, evolution and experience*, *J. Phys. Conf. Ser.* **331** (2011) 032023.
- [51] M. Pivk and F. R. Le Diberder, *sPlot: A statistical tool to unfold data distributions*, *Nucl. Instrum. Meth.* **A555** (2005) 356, [arXiv:physics/0402083](https://arxiv.org/abs/physics/0402083).
- [52] M. Abadi *et al.*, *TensorFlow: Large-scale machine learning on heterogeneous systems*, 2015. Software available from tensorflow.org.
- [53] F. Chollet *et al.*, *Keras*, <https://keras.io>, 2015.
- [54] M. Borisyak and N. Kazeev, *Machine Learning on data with sPlot background subtraction*, *JINST* **14** (2019) P08020, [arXiv:1905.11719](https://arxiv.org/abs/1905.11719).
- [55] G. A. Cowan, D. C. Craik, and M. D. Needham, *RapidSim: an application for the fast simulation of heavy-quark hadron decays*, *Comput. Phys. Commun.* **214** (2017) 239, [arXiv:1612.07489](https://arxiv.org/abs/1612.07489).
- [56] L. Breiman, J. H. Friedman, R. A. Olshen, and C. J. Stone, *Classification and regression trees*, Wadsworth international group, Belmont, California, USA, 1984.
- [57] Y. Freund and R. E. Schapire, *A decision-theoretic generalization of on-line learning and an application to boosting*, *J. Comput. Syst. Sci.* **55** (1997) 119.
- [58] F. Pedregosa *et al.*, *Scikit-learn: Machine learning in Python*, *J. Machine Learning Res.* **12** (2011) 2825, [arXiv:1201.0490](https://arxiv.org/abs/1201.0490), and online at <http://scikit-learn.org/stable/>.
- [59] L. Prokhorenkova *et al.*, *Catboost: unbiased boosting with categorical features*, [arXiv:1706.09516](https://arxiv.org/abs/1706.09516).
- [60] G. Punzi, *Sensitivity of searches for new signals and its optimization*, eConf **C030908** (2003) MODT002, [arXiv:physics/0308063](https://arxiv.org/abs/physics/0308063).
- [61] J. M. Blatt and V. F. Weisskopf, *Theoretical nuclear physics*, Springer, New York, 1952.
- [62] S. S. Wilks, *The large-sample distribution of the likelihood ratio for testing composite hypotheses*, *Ann. Math. Stat.* **9** (1938) 60.
- [63] LHCb collaboration, R. Aaij *et al.*, *Precision measurement of D meson mass differences*, *JHEP* **06** (2013) 065, [arXiv:1304.6865](https://arxiv.org/abs/1304.6865).

K. De Bruyn⁷⁹ ID, S. De Capua⁶³ ID, M. De Cian²² ID, U. De Freitas Carneiro Da Graca^{2,a} ID, E. De Lucia²⁸ ID, J.M. De Miranda² ID, L. De Paula³ ID, M. De Serio^{24,f} ID, P. De Simone²⁸ ID, F. De Vellis¹⁹ ID, J.A. de Vries⁸⁰ ID, F. Debernardis²⁴ ID, D. Decamp¹⁰ ID, V. Dedu¹³ ID, S. Dekkers¹ ID, L. Del Buono¹⁶ ID, B. Delaney⁶⁵ ID, H.-P. Dembinski¹⁹ ID, J. Deng⁸ ID, V. Denysenko⁵¹ ID, O. Deschamps¹¹ ID, F. Dettori^{32,i} ID, B. Dey⁷⁷ ID, P. Di Nezza²⁸ ID, I. Diachkov⁴⁴ ID, S. Didenko⁴⁴ ID, S. Ding⁶⁹ ID, L. Dittmann²² ID, V. Dobishuk⁵³ ID, A. D. Docheva⁶⁰ ID, C. Dong^{4,b} ID, A.M. Donohoe²³ ID, F. Dordei³² ID, A.C. dos Reis² ID, A. D. Dowling⁶⁹ ID, W. Duan⁷² ID, P. Duda⁸¹ ID, M.W. Dudek⁴¹ ID, L. Dufour⁴⁹ ID, V. Duk³⁴ ID, P. Durante⁴⁹ ID, M. M. Duras⁸¹ ID, J.M. Durham⁶⁸ ID, O. D. Durmus⁷⁷ ID, A. Dziurda⁴¹ ID, A. Dzyuba⁴⁴ ID, S. Easo⁵⁸ ID, E. Eckstein¹⁸ ID, U. Egede¹ ID, A. Egorychev⁴⁴ ID, V. Egorychev⁴⁴ ID, S. Eisenhardt⁵⁹ ID, E. Ejopu⁶³ ID, L. Eklund⁸³ ID, M. Elashri⁶⁶ ID, J. Ellbracht¹⁹ ID, S. Ely⁶² ID, A. Ene⁴³ ID, J. Eschle⁶⁹ ID, S. Esen²² ID, T. Evans³⁸ ID, F. Fabiano³² ID, S. Faghah⁶⁶ ID, L.N. Falcao² ID, Y. Fan⁷ ID, B. Fang⁷ ID, L. Fantini^{34,p,49} ID, M. Faria⁵⁰ ID, K. Farmer⁵⁹ ID, D. Fazzini^{31,n} ID, L. Felkowski⁸¹ ID, M. Feng^{5,7} ID, M. Feo² ID, A. Fernandez Casani⁴⁸ ID, M. Fernandez Gomez⁴⁷ ID, A.D. Fernez⁶⁷ ID, F. Ferrari^{25,h} ID, F. Ferreira Rodrigues³ ID, M. Ferrillo⁵¹ ID, M. Ferro-Luzzi⁴⁹ ID, S. Filippov⁴⁴ ID, R.A. Fini²⁴ ID, M. Fiorini^{26,j} ID, M. Firlej⁴⁰ ID, K.L. Fischer⁶⁴ ID, D.S. Fitzgerald⁸⁵ ID, C. Fitzpatrick⁶³ ID, T. Fiutowski⁴⁰ ID, F. Fleuret¹⁵ ID, M. Fontana²⁵ ID, L. F. Foreman⁶³ ID, R. Forty⁴⁹ ID, D. Foulds-Holt⁵⁶ ID, V. Franco Lima³ ID, M. Franco Sevilla⁶⁷ ID, M. Frank⁴⁹ ID, E. Franzoso^{26,j} ID, G. Frau⁶³ ID, C. Frei⁴⁹ ID, D.A. Friday⁶³ ID, J. Fu⁷ ID, Q. Führing^{19,e,56} ID, Y. Fujii¹ ID, T. Fulghesu¹³ ID, E. Gabriel³⁸ ID, G. Galati²⁴ ID, M.D. Galati³⁸ ID, A. Gallas Torreira⁴⁷ ID, D. Galli^{25,h} ID, S. Gambetta⁵⁹ ID, M. Gandelman³ ID, P. Gandini³⁰ ID, B. Ganie⁶³ ID, H. Gao⁷ ID, R. Gao⁶⁴ ID, T.Q. Gao⁵⁶ ID, Y. Gao⁸ ID, Y. Gao⁶ ID, Y. Gao⁸ ID, L.M. Garcia Martin⁵⁰ ID, P. Garcia Moreno⁴⁶ ID, J. García Pardiñas⁴⁹ ID, P. Gardner⁶⁷ ID, K. G. Garg⁸ ID, L. Garrido⁴⁶ ID, C. Gaspar⁴⁹ ID, A. Gavrikov³³ ID, L.L. Gerken¹⁹ ID, E. Gersabeck⁶³ ID, M. Gersabeck²⁰ ID, T. Gershon⁵⁷ ID, S. Ghizzo^{29,l} ID, Z. Ghorbanimoghaddam⁵⁵ ID, L. Giambastiani^{33,o} ID, F. I. Giasemis^{16,d} ID, V. Gibson⁵⁶ ID, H.K. Giemza⁴² ID, A.L. Gilman⁶⁴ ID, M. Giovannetti²⁸ ID, A. Gioventù⁴⁶ ID, L. Girardey^{63,58} ID, C. Giugliano^{26,j} ID, M.A. Giza⁴¹ ID, F.C. Glaser^{14,22} ID, V.V. Gligorov^{16,49} ID, C. Göbel⁷⁰ ID, L. Golinka-Bezshyyko⁸⁴ ID, E. Golobardes⁴⁵ ID, D. Golubkov⁴⁴ ID, A. Golutvin^{62,49} ID, S. Gomez Fernandez⁴⁶ ID, W. Gomulka⁴⁰ ID, F. Goncalves Abrantes⁶⁴ ID, M. Goncerz⁴¹ ID, G. Gong^{4,b} ID, J. A. Gooding¹⁹ ID, I.V. Gorelov⁴⁴ ID, C. Gotti³¹ ID, E. Govorkova⁶⁵ ID, J.P. Grabowski¹⁸ ID, L.A. Granado Cardoso⁴⁹ ID, E. Graugés⁴⁶ ID, E. Graverini^{50,r} ID, L. Grazette⁵⁷ ID, G. Graziani ID, A. T. Grecu⁴³ ID, L.M. Greeven³⁸ ID, N.A. Grieser⁶⁶ ID, L. Grillo⁶⁰ ID, S. Gromov⁴⁴ ID, C. Gu¹⁵ ID, M. Guarise²⁶ ID, L. Guerry¹¹ ID, V. Guliaeva⁴⁴ ID, P. A. Günther²² ID, A.-K. Guseinov⁵⁰ ID, E. Gushchin⁴⁴ ID, Y. Guz^{6,49} ID, T. Gys⁴⁹ ID, K. Habermann¹⁸ ID, T. Hadavizadeh¹ ID, C. Hadjivasiliou⁶⁷ ID, G. Haefeli⁵⁰ ID, C. Haen⁴⁹ ID, G. Hallett⁵⁷ ID, M.M. Halvorsen⁴⁹ ID, P.M. Hamilton⁶⁷ ID, J. Hammerich⁶¹ ID, Q. Han³³ ID, X. Han^{22,49} ID, S. Hansmann-Menzemer²² ID, L. Hao⁷ ID, N. Harnew⁶⁴ ID, T. H. Harris¹ ID, M. Hartmann¹⁴ ID, S. Hashmi⁴⁰ ID, J. He^{7,c} ID, F. Hemmer⁴⁹ ID, C. Henderson⁶⁶ ID, R.D.L. Henderson^{1,57} ID, A.M. Hennequin⁴⁹ ID, K. Hennessy⁶¹ ID, L. Henry⁵⁰ ID, J. Herd⁶² ID, P. Herrero Gascon²² ID, J. Heuel¹⁷ ID, A. Hicheur³ ID, G. Hijano Mendizabal⁵¹ ID, J. Horswill⁶³ ID, R. Hou⁸ ID, Y. Hou¹¹ ID, N. Howarth⁶¹ ID, J. Hu⁷² ID, W. Hu⁶ ID, X. Hu^{4,b} ID, W. Huang⁷ ID, W. Hulsbergen³⁸ ID, R.J. Hunter⁵⁷ ID, M. Hushchyn⁴⁴ ID, D. Hutchcroft⁶¹ ID, M. Idzik⁴⁰ ID, D. Ilin⁴⁴ ID, P. Ilten⁶⁶ ID, A. Inglessi⁴⁴ ID, A. Iniuikhin⁴⁴ ID, A. Ishteev⁴⁴ ID, K. Ivshin⁴⁴ ID, R. Jacobsson⁴⁹ ID, H. Jage¹⁷ ID, S.J. Jaimes Elles^{75,49,48} ID, S. Jakobsen⁴⁹ ID, E. Jans³⁸ ID, B.K. Jashal⁴⁸ ID, A. Jawahery⁶⁷ ID, V. Jevtic^{19,e} ID, E. Jiang⁶⁷ ID, X. Jiang^{5,7} ID, Y. Jiang⁷ ID, Y. J. Jiang⁶ ID, M. John⁶⁴ ID, A. John Rubesh Rajan²³ ID, D. Johnson⁵⁴ ID, C.R. Jones⁵⁶ ID, T.P. Jones⁵⁷ ID, S. Joshi⁴² ID, B. Jost⁴⁹ ID, J. Juan Castella⁵⁶ ID, N. Jurik⁴⁹ ID, I. Juszczak⁴¹ ID, D. Kaminaris⁵⁰ ID, S. Kandybei⁵² ID, M. Kane⁵⁹ ID, Y. Kang^{4,b} ID, C. Kar¹¹ ID,

C.J.G. Onderwater⁸⁰ ID, R.H. O'Neil⁴⁹ ID, D. Osthues¹⁹ ID, J.M. Otalora Goicochea³ ID,
 P. Owen⁵¹ ID, A. Oyanguren⁴⁸ ID, O. Ozcelik⁵⁹ ID, F. Paciolla^{35,u} ID, A. Padee⁴² ID,
 K.O. Padeken¹⁸ ID, B. Pagare⁵⁷ ID, T. Pajero⁴⁹ ID, A. Palano²⁴ ID, M. Palutan²⁸ ID, X.
 Pan^{4,b} ID, G. Panshin⁵ ID, L. Paolucci⁵⁷ ID, A. Papanestis^{58,49} ID, M. Pappagallo^{24,f} ID,
 L.L. Pappalardo²⁶ ID, C. Pappenheimer⁶⁶ ID, C. Parkes⁶³ ID, D. Parmar⁷⁶ ID,
 B. Passalacqua^{26,j} ID, G. Passaleva²⁷ ID, D. Passaro^{35,q,49} ID, A. Pastore²⁴ ID, M. Patel⁶² ID,
 J. Patoc⁶⁴ ID, C. Patrignani^{25,h} ID, A. Paul⁶⁹ ID, C.J. Pawley⁸⁰ ID, A. Pellegrino³⁸ ID, J.
 Peng^{5,7} ID, M. Pepe Altarelli²⁸ ID, S. Perazzini²⁵ ID, D. Pereima⁴⁴ ID, H. Pereira Da Costa⁶⁸ ID,
 A. Pereiro Castro⁴⁷ ID, P. Perret¹¹ ID, A. Perrevoort⁷⁹ ID, A. Perro^{49,13} ID, M.J. Peters⁶⁶ ID,
 K. Petridis⁵⁵ ID, A. Petrolini^{29,l} ID, J. P. Pfaller⁶⁶ ID, H. Pham⁶⁹ ID, L. Pica³⁵ ID,
 M. Piccini³⁴ ID, L. Piccolo³² ID, B. Pietrzyk¹⁰ ID, G. Pietrzyk¹⁴ ID, R. N. Pilato⁶¹ ID,
 D. Pinci³⁶ ID, F. Pisani⁴⁹ ID, M. Pizzichemi^{31,n,49} ID, V. Placinta⁴³ ID, M. Plo Casasus⁴⁷ ID,
 T. Poeschl⁴⁹ ID, F. Polci¹⁶ ID, M. Poli Lener²⁸ ID, A. Poluektov¹³ ID, N. Polukhina⁴⁴ ID,
 I. Polyakov⁶³ ID, E. Polycarpo³ ID, S. Ponce⁴⁹ ID, D. Popov^{7,49} ID, S. Poslavskii⁴⁴ ID,
 K. Prasant⁵⁹ ID, C. Prouve⁸² ID, D. Provenzano^{32,i} ID, V. Pugatch⁵³ ID, G. Punzi^{35,r} ID, S.
 Qasim⁵¹ ID, Q. Q. Qian⁶ ID, W. Qian⁷ ID, N. Qin^{4,b} ID, S. Qu^{4,b} ID, R. Quagliani⁴⁹ ID,
 R.I. Rabadan Trejo⁵⁷ ID, J.H. Rademacker⁵⁵ ID, M. Rama³⁵ ID, M. Ramírez García⁸⁵ ID,
 V. Ramos De Oliveira⁷⁰ ID, M. Ramos Pernas⁵⁷ ID, M.S. Rangel³ ID, F. Ratnikov⁴⁴ ID,
 G. Raven³⁹ ID, M. Rebollo De Miguel⁴⁸ ID, F. Redi^{30,g} ID, J. Reich⁵⁵ ID, F. Reiss²⁰ ID, Z. Ren⁷ ID,
 P.K. Resmi⁶⁴ ID, M. Ribalda Galvez⁴⁶ ID, R. Ribatti⁵⁰ ID, G. Ricart^{15,12} ID, D. Riccardi^{35,q} ID,
 S. Ricciardi⁵⁸ ID, K. Richardson⁶⁵ ID, M. Richardson-Slipper⁵⁹ ID, K. Rinnert⁶¹ ID,
 P. Robbe^{14,49} ID, G. Robertson⁶⁰ ID, E. Rodrigues⁶¹ ID, A. Rodriguez Alvarez⁴⁶ ID,
 E. Rodriguez Fernandez⁴⁷ ID, J.A. Rodriguez Lopez⁷⁵ ID, E. Rodriguez Rodriguez⁴⁹ ID,
 J. Roensch¹⁹ ID, A. Rogachev⁴⁴ ID, A. Rogovskiy⁵⁸ ID, D.L. Rolf¹⁹ ID, P. Roloff⁴⁹ ID,
 V. Romanovskiy⁶⁶ ID, A. Romero Vidal⁴⁷ ID, G. Romolini²⁶ ID, F. Ronchetti⁵⁰ ID, T. Rong⁶ ID,
 M. Rotondo²⁸ ID, S. R. Roy²² ID, M.S. Rudolph⁶⁹ ID, M. Ruiz Diaz²² ID,
 R.A. Ruiz Fernandez⁴⁷ ID, J. Ruiz Vidal⁸⁰ ID, J. Ryzka⁴⁰ ID, J. J. Saavedra-Arias⁹ ID,
 J.J. Saborido Silva⁴⁷ ID, R. Sadek¹⁵ ID, N. Sagidova⁴⁴ ID, D. Sahoo⁷⁷ ID, N. Sahoo⁵⁴ ID,
 B. Saitta^{32,i} ID, M. Salomoni^{31,49,n} ID, I. Sanderswood⁴⁸ ID, R. Santacesaria³⁶ ID,
 C. Santamarina Rios⁴⁷ ID, M. Santimaria²⁸ ID, L. Santoro² ID, E. Santovetti³⁷ ID,
 A. Saputi^{26,49} ID, D. Saranin⁴⁴ ID, A. Sarnatskiy⁷⁹ ID, G. Sarpis⁵⁹ ID, M. Sarpis⁷⁸ ID,
 C. Satriano^{36,s} ID, A. Satta³⁷ ID, M. Saur⁷³ ID, D. Savrina⁴⁴ ID, H. Sazak¹⁷ ID,
 F. Sborzacchi^{49,28} ID, A. Scarabotto¹⁹ ID, S. Schael¹⁷ ID, S. Scherl⁶¹ ID, M. Schiller⁶⁰ ID,
 H. Schindler⁴⁹ ID, M. Schmelling²¹ ID, B. Schmidt⁴⁹ ID, S. Schmitt¹⁷ ID, H. Schmitz¹⁸,
 O. Schneider⁵⁰ ID, A. Schopper⁶² ID, N. Schulte¹⁹ ID, S. Schulte⁵⁰ ID, M.H. Schune¹⁴ ID,
 G. Schwering¹⁷ ID, B. Sciascia²⁸ ID, A. Sciuccati⁴⁹ ID, I. Segal⁷⁶ ID, S. Sellam⁴⁷ ID,
 A. Semennikov⁴⁴ ID, T. Senger⁵¹ ID, M. Senghi Soares³⁹ ID, A. Sergi^{29,l} ID, N. Serra⁵¹ ID,
 L. Sestini²⁷ ID, A. Seuthe¹⁹ ID, Y. Shang⁶ ID, D.M. Shangase⁸⁵ ID, M. Shapkin⁴⁴ ID, R. S.
 Sharma⁶⁹ ID, I. Shchemerov⁴⁴ ID, L. Shchutska⁵⁰ ID, T. Shears⁶¹ ID, L. Shekhtman⁴⁴ ID,
 Z. Shen³⁸ ID, S. Sheng^{5,7} ID, V. Shevchenko⁴⁴ ID, B. Shi⁷ ID, Q. Shi⁷ ID, Y. Shimizu¹⁴ ID,
 E. Shmanin²⁵ ID, R. Shorkin⁴⁴ ID, J.D. Shupperd⁶⁹ ID, R. Silva Coutinho⁶⁹ ID, G. Simi^{33,o} ID,
 S. Simone^{24,f} ID, M. Singha⁷⁷ ID, N. Skidmore⁵⁷ ID, T. Skwarnicki⁶⁹ ID, M.W. Slater⁵⁴ ID,
 E. Smith⁶⁵ ID, K. Smith⁶⁸ ID, M. Smith⁶² ID, A. Snoch³⁸ ID, L. Soares Lavra⁵⁹ ID,
 M.D. Sokoloff⁶⁶ ID, F.J.P. Soler⁶⁰ ID, A. Solomin⁵⁵ ID, A. Solovev⁴⁴ ID, I. Solovyev⁴⁴ ID, N. S.
 Sommerfeld¹⁸ ID, R. Song¹ ID, Y. Song⁵⁰ ID, Y. Song^{4,b} ID, Y. S. Song⁶ ID,
 F.L. Souza De Almeida⁶⁹ ID, B. Souza De Paula³ ID, E. Spadaro Norella^{29,l} ID, E. Spedicato²⁵ ID,
 J.G. Speer¹⁹ ID, E. Spiridenkov⁴⁴ ID, P. Spradlin⁶⁰ ID, V. Sriskaran⁴⁹ ID, F. Stagni⁴⁹ ID,
 M. Stahl⁷⁶ ID, S. Stahl⁴⁹ ID, S. Stanislaus⁶⁴ ID, M. Stefaniak⁸⁶ ID, E.N. Stein⁴⁹ ID,
 O. Steinkamp⁵¹ ID, O. Stenyakin⁴⁴ ID, H. Stevens¹⁹ ID, D. Strekalina⁴⁴ ID, Y. Su⁷ ID, F. Suljik⁶⁴ ID,
 J. Sun³² ID, L. Sun⁷⁴ ID, D. Sundfeld² ID, W. Sutcliffe⁵¹ ID, K. Swientek⁴⁰ ID, F. Swystun⁵⁶ ID,

- A. Szabelski⁴² , T. Szumlak⁴⁰ , Y. Tan^{4,b} , Y. Tang⁷⁴ , M.D. Tat²² , A. Terentev⁴⁴ , F. Terzuoli^{35,u,49} , F. Teubert⁴⁹ , E. Thomas⁴⁹ , D.J.D. Thompson⁵⁴ , H. Tilquin⁶² , V. Tisserand¹¹ , S. T'Jampens¹⁰ , M. Tobin^{5,49} , L. Tomassetti^{26,j} , G. Tonani^{30,m} , X. Tong⁶ , T. Tork³⁰ , D. Torres Machado² , L. Toscano¹⁹ , D.Y. Tou^{4,b} , C. Trippl⁴⁵ , G. Tuci²² , N. Tuning³⁸ , L.H. Uecker²² , A. Ukleja⁴⁰ , D.J. Unverzagt²² , A. Upadhyay⁷⁷ , B. Urbach⁵⁹ , A. Usachov³⁹ , A. Ustyuzhanin⁴⁴ , U. Uwer²² , V. Vagnoni²⁵ , V. Valcarce Cadenas⁴⁷ , G. Valenti²⁵ , N. Valls Canudas⁴⁹ , J. van Eldik⁴⁹ , H. Van Hecke⁶⁸ , E. van Herwijnen⁶² , C.B. Van Hulse^{47,x} , R. Van Laak⁵⁰ , M. van Veghel³⁸ , G. Vasquez⁵¹ , R. Vazquez Gomez⁴⁶ , P. Vazquez Regueiro⁴⁷ , C. Vázquez Sierra⁸² , S. Vecchi²⁶ , J.J. Velthuis⁵⁵ , M. Veltri^{27,v} , A. Venkateswaran⁵⁰ , M. Verdoglia³² , M. Vesterinen⁵⁷ , D. Vico Benet⁶⁴ , P. Vidrier Villalba⁴⁶ , M. Vieites Diaz⁴⁷ , X. Vilasis-Cardona⁴⁵ , E. Vilella Figueras⁶¹ , A. Villa²⁵ , P. Vincent¹⁶ , B. Vivacqua³ , F.C. Volle⁵⁴ , D. vom Bruch¹³ , N. Voropaev⁴⁴ , K. Vos⁸⁰ , C. Vrachas⁵⁹ , J. Wagner¹⁹ , J. Walsh³⁵ , E.J. Walton^{1,57} , G. Wan⁶ , A. Wang⁷ , C. Wang²² , G. Wang⁸ , H. Wang⁷³ , J. Wang⁶ , J. Wang⁵ , J. Wang^{4,b} , J. Wang⁷⁴ , M. Wang⁴⁹ , N. W. Wang⁷ , R. Wang⁵⁵ , X. Wang⁸ , X. Wang⁷² , X. W. Wang⁶² , Y. Wang⁶ , Y. W. Wang⁷³ , Z. Wang¹⁴ , Z. Wang^{4,b} , Z. Wang³⁰ , J.A. Ward^{57,1} , M. Waterlaat⁴⁹ , N.K. Watson⁵⁴ , D. Websdale⁶² , Y. Wei⁶ , J. Wendel⁸² , B.D.C. Westhenry⁵⁵ , C. White⁵⁶ , M. Whitehead⁶⁰ , E. Whiter⁵⁴ , A.R. Wiederhold⁶³ , D. Wiedner¹⁹ , G. Wilkinson⁶⁴ , M.K. Wilkinson⁶⁶ , M. Williams⁶⁵ , M. J. Williams⁴⁹ , M.R.J. Williams⁵⁹ , R. Williams⁵⁶ , Z. Williams⁵⁵ , F.F. Wilson⁵⁸ , M. Winn¹² , W. Wislicki⁴² , M. Witek⁴¹ , L. Witola¹⁹ , G. Wormser¹⁴ , S.A. Wotton⁵⁶ , H. Wu⁶⁹ , J. Wu⁸ , X. Wu⁷⁴ , Y. Wu^{6,56} , Z. Wu⁷ , K. Wyllie⁴⁹ , S. Xian⁷² , Z. Xiang⁵ , Y. Xie⁸ , T. X. Xing³⁰ , A. Xu³⁵ , L. Xu^{4,b} , L. Xu^{4,b} , M. Xu⁵⁷ , Z. Xu⁴⁹ , Z. Xu⁷ , Z. Xu⁵ , K. Yang⁶² , S. Yang⁷ , X. Yang⁶ , Y. Yang^{29,l} , Z. Yang⁶ , V. Yeroshenko¹⁴ , H. Yeung⁶³ , H. Yin⁸ , X. Yin⁷ , C. Y. Yu⁶ , J. Yu⁷¹ , X. Yuan⁵ , Y. Yuan^{5,7} , E. Zaffaroni⁵⁰ , M. Zavertyaev²¹ , M. Zdybal⁴¹ , F. Zenesini²⁵ , C. Zeng^{5,7} , M. Zeng^{4,b} , C. Zhang⁶ , D. Zhang⁸ , J. Zhang⁷ , L. Zhang^{4,b} , S. Zhang⁷¹ , S. Zhang⁶⁴ , Y. Zhang⁶ , Y. Z. Zhang^{4,b} , Z. Zhang^{4,b} , Y. Zhao²² , A. Zhelezov²² , S. Z. Zheng⁶ , X. Z. Zheng^{4,b} , Y. Zheng⁷ , T. Zhou⁶ , X. Zhou⁸ , Y. Zhou⁷ , V. Zhovkovska⁵⁷ , L. Z. Zhu⁷ , X. Zhu^{4,b} , X. Zhu⁸ , Y. Zhu¹⁷ , V. Zhukov¹⁷ , J. Zhuo⁴⁸ , Q. Zou^{5,7} , D. Zuliani^{33,o} , G. Zunica⁵⁰

¹School of Physics and Astronomy, Monash University, Melbourne, Australia

²Centro Brasileiro de Pesquisas Físicas (CBPF), Rio de Janeiro, Brazil

³Universidade Federal do Rio de Janeiro (UFRJ), Rio de Janeiro, Brazil

⁴Department of Engineering Physics, Tsinghua University, Beijing, China

⁵Institute Of High Energy Physics (IHEP), Beijing, China

⁶School of Physics State Key Laboratory of Nuclear Physics and Technology, Peking University, Beijing, China

⁷University of Chinese Academy of Sciences, Beijing, China

⁸Institute of Particle Physics, Central China Normal University, Wuhan, Hubei, China

⁹Consejo Nacional de Rectores (CONARE), San Jose, Costa Rica

¹⁰Université Savoie Mont Blanc, CNRS, IN2P3-LAPP, Annecy, France

¹¹Université Clermont Auvergne, CNRS/IN2P3, LPC, Clermont-Ferrand, France

¹²Université Paris-Saclay, Centre d'Etudes de Saclay (CEA), IRFU, Saclay, France, Gif-Sur-Yvette, France

¹³Aix Marseille Univ, CNRS/IN2P3, CPPM, Marseille, France

¹⁴Université Paris-Saclay, CNRS/IN2P3, IJCLab, Orsay, France

¹⁵Laboratoire Leprince-Ringuet, CNRS/IN2P3, Ecole Polytechnique, Institut Polytechnique de Paris, Palaiseau, France

- ¹⁶*LPNHE, Sorbonne Université, Paris Diderot Sorbonne Paris Cité, CNRS/IN2P3, Paris, France*
- ¹⁷*I. Physikalisches Institut, RWTH Aachen University, Aachen, Germany*
- ¹⁸*Universität Bonn - Helmholtz-Institut für Strahlen und Kernphysik, Bonn, Germany*
- ¹⁹*Fakultät Physik, Technische Universität Dortmund, Dortmund, Germany*
- ²⁰*Physikalisches Institut, Albert-Ludwigs-Universität Freiburg, Freiburg, Germany*
- ²¹*Max-Planck-Institut für Kernphysik (MPIK), Heidelberg, Germany*
- ²²*Physikalisches Institut, Ruprecht-Karls-Universität Heidelberg, Heidelberg, Germany*
- ²³*School of Physics, University College Dublin, Dublin, Ireland*
- ²⁴*INFN Sezione di Bari, Bari, Italy*
- ²⁵*INFN Sezione di Bologna, Bologna, Italy*
- ²⁶*INFN Sezione di Ferrara, Ferrara, Italy*
- ²⁷*INFN Sezione di Firenze, Firenze, Italy*
- ²⁸*INFN Laboratori Nazionali di Frascati, Frascati, Italy*
- ²⁹*INFN Sezione di Genova, Genova, Italy*
- ³⁰*INFN Sezione di Milano, Milano, Italy*
- ³¹*INFN Sezione di Milano-Bicocca, Milano, Italy*
- ³²*INFN Sezione di Cagliari, Monserrato, Italy*
- ³³*INFN Sezione di Padova, Padova, Italy*
- ³⁴*INFN Sezione di Perugia, Perugia, Italy*
- ³⁵*INFN Sezione di Pisa, Pisa, Italy*
- ³⁶*INFN Sezione di Roma La Sapienza, Roma, Italy*
- ³⁷*INFN Sezione di Roma Tor Vergata, Roma, Italy*
- ³⁸*Nikhef National Institute for Subatomic Physics, Amsterdam, Netherlands*
- ³⁹*Nikhef National Institute for Subatomic Physics and VU University Amsterdam, Amsterdam, Netherlands*
- ⁴⁰*AGH - University of Krakow, Faculty of Physics and Applied Computer Science, Kraków, Poland*
- ⁴¹*Henryk Niewodniczanski Institute of Nuclear Physics Polish Academy of Sciences, Kraków, Poland*
- ⁴²*National Center for Nuclear Research (NCBJ), Warsaw, Poland*
- ⁴³*Horia Hulubei National Institute of Physics and Nuclear Engineering, Bucharest-Magurele, Romania*
- ⁴⁴*Authors affiliated with an institute formerly covered by a cooperation agreement with CERN.*
- ⁴⁵*DS4DS, La Salle, Universitat Ramon Llull, Barcelona, Spain*
- ⁴⁶*ICCUB, Universitat de Barcelona, Barcelona, Spain*
- ⁴⁷*Instituto Galego de Física de Altas Enerxías (IGFAE), Universidade de Santiago de Compostela, Santiago de Compostela, Spain*
- ⁴⁸*Instituto de Física Corpuscular, Centro Mixto Universidad de Valencia - CSIC, Valencia, Spain*
- ⁴⁹*European Organization for Nuclear Research (CERN), Geneva, Switzerland*
- ⁵⁰*Institute of Physics, Ecole Polytechnique Fédérale de Lausanne (EPFL), Lausanne, Switzerland*
- ⁵¹*Physik-Institut, Universität Zürich, Zürich, Switzerland*
- ⁵²*NSC Kharkiv Institute of Physics and Technology (NSC KIPT), Kharkiv, Ukraine*
- ⁵³*Institute for Nuclear Research of the National Academy of Sciences (KINR), Kyiv, Ukraine*
- ⁵⁴*School of Physics and Astronomy, University of Birmingham, Birmingham, United Kingdom*
- ⁵⁵*H.H. Wills Physics Laboratory, University of Bristol, Bristol, United Kingdom*
- ⁵⁶*Cavendish Laboratory, University of Cambridge, Cambridge, United Kingdom*
- ⁵⁷*Department of Physics, University of Warwick, Coventry, United Kingdom*
- ⁵⁸*STFC Rutherford Appleton Laboratory, Didcot, United Kingdom*
- ⁵⁹*School of Physics and Astronomy, University of Edinburgh, Edinburgh, United Kingdom*
- ⁶⁰*School of Physics and Astronomy, University of Glasgow, Glasgow, United Kingdom*
- ⁶¹*Oliver Lodge Laboratory, University of Liverpool, Liverpool, United Kingdom*
- ⁶²*Imperial College London, London, United Kingdom*
- ⁶³*Department of Physics and Astronomy, University of Manchester, Manchester, United Kingdom*
- ⁶⁴*Department of Physics, University of Oxford, Oxford, United Kingdom*
- ⁶⁵*Massachusetts Institute of Technology, Cambridge, MA, United States*
- ⁶⁶*University of Cincinnati, Cincinnati, OH, United States*
- ⁶⁷*University of Maryland, College Park, MD, United States*
- ⁶⁸*Los Alamos National Laboratory (LANL), Los Alamos, NM, United States*
- ⁶⁹*Syracuse University, Syracuse, NY, United States*

- ⁷⁰*Pontifícia Universidade Católica do Rio de Janeiro (PUC-Rio), Rio de Janeiro, Brazil, associated to* ³
- ⁷¹*School of Physics and Electronics, Hunan University, Changsha City, China, associated to* ⁸
- ⁷²*Guangdong Provincial Key Laboratory of Nuclear Science, Guangdong-Hong Kong Joint Laboratory of Quantum Matter, Institute of Quantum Matter, South China Normal University, Guangzhou, China, associated to* ⁴
- ⁷³*Lanzhou University, Lanzhou, China, associated to* ⁵
- ⁷⁴*School of Physics and Technology, Wuhan University, Wuhan, China, associated to* ⁴
- ⁷⁵*Departamento de Fisica , Universidad Nacional de Colombia, Bogota, Colombia, associated to* ¹⁶
- ⁷⁶*Ruhr Universitaet Bochum, Fakultaet f. Physik und Astronomie, Bochum, Germany, associated to* ¹⁹
- ⁷⁷*Eotvos Lorand University, Budapest, Hungary, associated to* ⁴⁹
- ⁷⁸*Vilnius University, Vilnius, Lithuania, associated to* ²⁰
- ⁷⁹*Van Swinderen Institute, University of Groningen, Groningen, Netherlands, associated to* ³⁸
- ⁸⁰*Universiteit Maastricht, Maastricht, Netherlands, associated to* ³⁸
- ⁸¹*Tadeusz Kosciuszko Cracow University of Technology, Cracow, Poland, associated to* ⁴¹
- ⁸²*Universidade da Coruña, A Coruña, Spain, associated to* ⁴⁵
- ⁸³*Department of Physics and Astronomy, Uppsala University, Uppsala, Sweden, associated to* ⁶⁰
- ⁸⁴*Taras Schevchenko University of Kyiv, Faculty of Physics, Kyiv, Ukraine, associated to* ¹⁴
- ⁸⁵*University of Michigan, Ann Arbor, MI, United States, associated to* ⁶⁹
- ⁸⁶*Ohio State University, Columbus, United States, associated to* ⁶⁸

^a*Centro Federal de Educacão Tecnológica Celso Suckow da Fonseca, Rio De Janeiro, Brazil*

^b*Center for High Energy Physics, Tsinghua University, Beijing, China*

^c*Hangzhou Institute for Advanced Study, UCAS, Hangzhou, China*

^d*LIP6, Sorbonne Université, Paris, France*

^e*Lamarr Institute for Machine Learning and Artificial Intelligence, Dortmund, Germany*

^f*Università di Bari, Bari, Italy*

^g*Università di Bergamo, Bergamo, Italy*

^h*Università di Bologna, Bologna, Italy*

ⁱ*Università di Cagliari, Cagliari, Italy*

^j*Università di Ferrara, Ferrara, Italy*

^k*Università di Firenze, Firenze, Italy*

^l*Università di Genova, Genova, Italy*

^m*Università degli Studi di Milano, Milano, Italy*

ⁿ*Università degli Studi di Milano-Bicocca, Milano, Italy*

^o*Università di Padova, Padova, Italy*

^p*Università di Perugia, Perugia, Italy*

^q*Scuola Normale Superiore, Pisa, Italy*

^r*Università di Pisa, Pisa, Italy*

^s*Università della Basilicata, Potenza, Italy*

^t*Università di Roma Tor Vergata, Roma, Italy*

^u*Università di Siena, Siena, Italy*

^v*Università di Urbino, Urbino, Italy*

^w*Universidad de Ingeniería y Tecnología (UTEC), Lima, Peru*

^x*Universidad de Alcalá, Alcalá de Henares , Spain*

^y*Facultad de Ciencias Fisicas, Madrid, Spain*

[†]*Deceased*